Thermoreversible cross-linking of maleated ethylene/propylene copolymers with diamines and amino-alcohols

M.A.J. van der Mee [a,b], J.G.P. Goossens [a,b,*], M. van Duin [c]

[a] *Laboratory of Polymer Technology, Department of Chemical Engineering and Chemistry, Eindhoven University of Technology, P.O. Box 513, 5600 MB Eindhoven, The Netherlands*
[b] *Dutch Polymer Institute, P.O. Box 902, 5600 AX Eindhoven, The Netherlands*
[c] *DSM Research, P.O. Box 18, 6160 MD Geleen, The Netherlands*

Abstract

Maleated ethylene/propylene copolymers (MAn-*g*-EPM) were thermoreversibly cross-linked using diamines and amino-alcohols. Covalent cross-links are formed via the equilibrium reaction of the grafted anhydride groups with di-functional cross-linkers containing combinations of primary (1°) and secondary (2°) amines and alcohols, while a shift of the equilibrium at elevated temperatures may result in their (partial) removal. Materials cross-linked with cross-linkers containing two 2° amine groups (2°–2°) and 2° amine and alcohol groups (2°–OH) are repeatedly processable via compression molding without chemical changes, which is an improvement in reversibility compared to the previously-studied cross-linking reactions with diols, for which irreversible side reactions limited the reversibility to some extent. The use of 1° amine groups results in materials that are not reprocessable via compression molding, due to irreversible imide formation. The 2°–2° and 2°–OH materials have higher levels of cross-linking after remolding than the diol-cross-linked MAn-*g*-EPM, which results in significant differences in rubber properties. Fourier transform infrared (FTIR) spectroscopy suggested that the reprocessability of these materials is caused by a continuous, dynamic exchange between cross-linked and free groups. Finally, the use of cross-linkers containing 3° amine groups results in the formation of ionic interactions. These materials are easily reprocessable at temperatures as low as 125 °C and have significantly different properties than the covalently cross-linked materials, due to the occurrence of ion hopping.
© 2008 Elsevier Ltd. All rights reserved.

Keywords: Thermoreversible cross-linking; Microphase separation; Mechanical properties

1. Introduction

Elastomers have to be cross-linked to obtain typical rubber properties, such as elasticity, toughness and solvent resistance. The main industrial rubber cross-linking techniques, i.e., sulfur vulcanization and peroxide cure, yield irreversible covalent cross-links, which prevent melt processing, thereby resulting in time-consuming, multi-step processing cycles [1]. This has

led to the development of thermoplastic elastomers (TPEs), which ideally combine the service properties of cross-linked elastomers with the melt processability of thermoplastics. The cross-links in TPEs are of thermoreversible nature; i.e., they weaken or disappear at elevated temperatures, thereby allowing flow, while they behave as irreversible cross-links at service temperature after cooling [2].

An interesting option to achieve TPE-like behavior is the use of thermoreversible *covalent* cross-links, using the inherent temperature dependence of equilibrium reactions. Covalent cross-links are formed via the forward reaction between suitable chemical functionalities at relatively low temperatures, while a shift in the equilibrium at elevated temperatures may result in their (partial) removal [3]. Complete reversibility is not

---

* Corresponding author. Laboratory of Polymer Technology, Department of Chemical Engineering and Chemistry, Eindhoven University of Technology, P.O. Box 513, 5600 MB Eindhoven, The Netherlands. Tel.: +31 40 2473899; fax: +31 40 2436999.

E-mail address: j.g.p.goossens@tue.nl (J.G.P. Goossens).

necessary, as only a sufficient number of chemical bonds need to be removed to permit adequate melt flow. The service properties of the thermoreversible network are expected to be similar to those of conventional, irreversibly cross-linked networks [3].

The Diels—Alder [4 + 2] cycloaddition is particularly suitable for this purpose, because of the readiness of Diels—Alder adducts to undergo the reverse reaction (retro-Diels—Alder) upon heating. Diels—Alder reactions between furan and maleimide groups [4,5] and between two cyclopentadiene groups [6,7] have been successfully used for thermoreversible cross-linking of polymers. Urethane formation from isocyanate and hydroxyl groups is also thermoreversible [8,9] and has been used for polymer cross-linking [10,11]. Previous work in our group showed that the reverse reaction at elevated temperatures results in the depolymerization of linear polyurethanes and in easy processability, provided that the molecular weights are not too high [12—14]. Nitroso dimerization [15], the reaction of azlactones with phenols [16] and the reaction of carboxylic acids with vinyl ethers [17] have also been applied to obtain thermoreversible polymer networks. Finally, the reactions of cyclic anhydrides with alcohols to form hemi-esters [18—21] or with amines to form amide—acids [22,23] have been reported to be thermoreversible.

During previous work in our group, the thermoreversible covalent cross-linking of maleated ethylene/propylene copolymer (MAn-g-EPM) with diols [24] was studied, while ionic interactions with metal cations [25] and hydrogen bonds combined with ionic interactions [26] were explored as well. MAn-g-EPM cross-linked with diols (Scheme 1A) was repeatedly processable

via compression molding, indicating that the cross-links are indeed thermoreversible. However, irreversible di-ester formation [27,28] occurred for the longer diols and partial evaporation of the shorter diols out of the rubber. Both effects lowered the level of cross-linking, which resulted in changes in the rubber properties. Fortunately, the extent of these effects was not too high to prevent further reprocessing.

This paper discusses our continuing work on the thermoreversible cross-linking of the same MAn-g-EPM, now using diamines and amino-alcohols, with the main aim to improve the thermoreversibility compared to cross-linking with diols [24]. As discussed above, the reaction of the anhydride groups of MAn-g-EPM with amines is also thermoreversible. The reaction with primary (1°) amines may be less suitable for thermoreversible cross-linking, as the initially-formed 1° amide—acids are prone to irreversible imide formation already at moderately elevated temperatures (Scheme 1B) [22,23,29,30]. The use of secondary (2°) amines results in a thermoreversible reaction, since imide formation is not possible (Scheme 1C). Therefore, covalent cross-links are formed for any combination of alcohol and 1° and 2° amine groups. Tertiary (3°) amines cannot react with cyclic anhydrides, but may be used to neutralize carboxylic acid groups [30,31]. Therefore, addition of cross-linkers containing 3° amines to MAn-g-EPM with (partially) hydrolyzed anhydride groups results in the introduction of ionic interactions with ammonium cations (Scheme 1D), which may result in thermoreversibility as well.

First, Fourier transform infrared (FTIR) spectroscopy is used to identify the chemical structures of the cross-linked materials as well as the conversion of the cross-linking reactions.
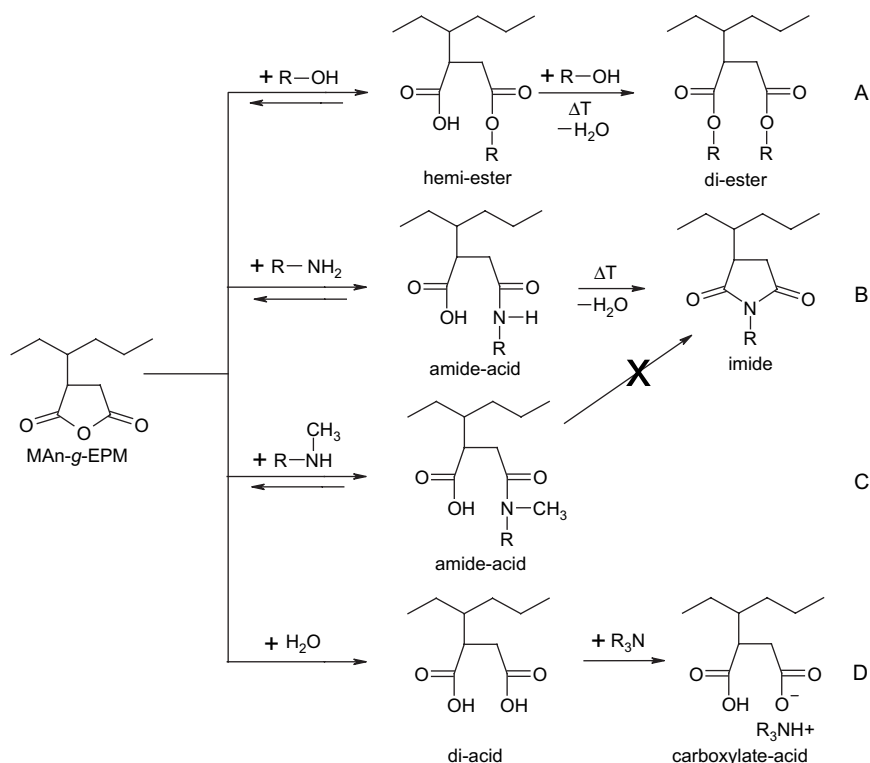
Scheme 1. Reaction scheme for the modification of MAn-g-EPM with alcohols or amines.

Note that the reaction with a diol is also studied here for reference. The cross-linked materials are compression molded at various temperatures to determine their reprocessability, while FTIR spectroscopy is used to study whether (undesired) reactions occur. The effects of the type of cross-linker on the morphology, as studied by small-angle X-ray scattering (SAXS) and dynamic mechanical thermal analysis (DMTA), and on the mechanical properties, i.e., hardness, tensile properties and compression set (CS), are studied for the reprocessable materials. Finally, selected covalently cross-linked materials are subjected to heating−cooling cycles during time-resolved FTIR experiments in order to elucidate the mechanism of reversibility at elevated temperatures.

2. Experimental

2.1. Materials

Maleated ethylene/propylene copolymer (MAn-g-EPM; 49 wt% ethylene, 49 wt% propylene and 2.1 wt% maleic anhydride (MAn); $M_n = 40$ kg/mol, $M_w = 90$ kg/mol) was provided by DSM Elastomers. It was dried for 1 h at 170 °C under reduced pressure with a low nitrogen flow prior to use to convert all carboxylic acid groups, formed upon hydrolysis, back to anhydride. Ethylenediamine (1°−1°), N-methylethylenediamine (1°−2°), N,N-dimethylethylenediamine (1°−3°), N,N'-dimethylethylenediamine (2°−2°), N,N,N'-trimethylethylenediamine (2°−3°), N,N,N',N'-tetramethylethylenediamine (3°−3°), ethanolamine (1°−OH), 2-(methylamino)ethanol (2°−OH), ethyleneglycol (OH−OH), N,N-dimethylethanolamine (OH−3°) and p-toluenesulfonic acid monohydrate (all purchased from Aldrich) and tetrahydrofuran (THF, Biosolve) were used as received.

2.2. Cross-linking of MAn-g-EPM

Typically, 15 g of MAn-g-EPM was dissolved in 150 g of THF at 60 °C, after which the solution was cooled down to room temperature. MAn-g-EPM was partially (around 50%) or fully hydrolyzed via exposure to water from air for prolonged time at room temperature prior to the modification reactions with cross-linkers containing one or two 3° amine groups, respectively. For the modification with the OH−OH cross-linker, 5 mol% of p-toluenesulfonic acid, based on the molar amount of anhydride groups, was added to the solution as a catalyst [24]. Next, 0.5 mol of (di-functional) cross-linker per mol of grafted anhydride, was added to the solution, which was stirred for at least 30 min. The resulting solution or gel was poured into a Teflon®-covered Petri dish and dried under a nitrogen flow for several days at room temperature, followed by drying under vacuum for one day at 50 °C.

The cross-linked materials were compression molded between Teflon® sheets for 30 min at 125 and 150 °C and for 20 min at 175 °C in a Collin press to determine the optimal reprocessing conditions. Samples were compression molded for 20 min at 175 °C for characterization purposes and reversibility experiments.

2.3. Fourier transform infrared (FTIR) spectroscopy

Compression-molded films were analyzed on a BioRad Excalibur 3000 spectrometer equipped with a Specac Golden Gate attenuated total reflection (ATR) setup over a spectral range from 650 to 4000 cm^{-1} at a resolution of 4 cm^{-1}, co-adding 20 scans. The conversion of the anhydride groups (X_{Anh}) is calculated from the integrated intensity of the *anti*-symmetric carbonyl stretching vibration band at 1785 cm^{-1} (A_{1785}) of the anhydride groups using the integrated intensity of the band at 1460 cm^{-1} (A_{1460}), originating from the overlapping *anti*-symmetric CH$_3$ bending and CH$_2$ scissoring vibrations of the EPM backbone, as internal reference:

$$X_{Anh} = \left(1 - \left(\frac{(A_{1785}/A_{1460})_{\text{cross-linked}}}{(A_{1785}/A_{1460})_{\text{MAn-}g\text{-EPM}}}\right)\right) \times 100\% \qquad (1)$$

Reversibility experiments were performed on thin (~ 100 μm) compression-molded films on a BioRad FTS6000 spectrometer equipped with a UMA500 FTIR microscope over a spectral range from 650 to 4000 cm^{-1} at a resolution of 2 cm^{-1}, co-adding 20 scans. Samples were measured on a zinc selenide disk in transmission mode with an exposed sample area of approximately 30 by 30 μm using a MCT detector. Samples were exposed to the temperature profile shown in Fig. 1 using a Linkam TMS600 hotstage.
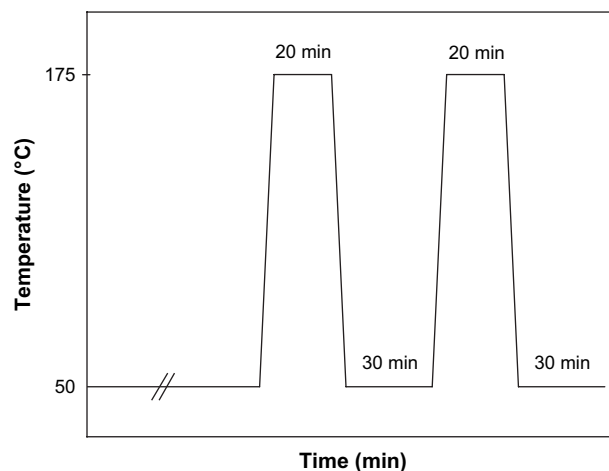

Fig. 1. Temperature profile for FTIR reversibility experiments.

2.4. Small-angle X-ray scattering (SAXS)

SAXS experiments were performed on compression-molded samples at the DUBBLE beamline (BM26) at the European Synchrotron Radiation Facility (ESRF) in Grenoble (France). The data were collected using a 2D multiwire gas-filled detector with pixel array dimensions of 512×512. The detector was positioned at 2.5 m from the sample and the q-scale was calibrated using the positions of diffracted peaks of silver behenate. The exposure time for each sample was 300 s and a wavelength of 1.2 Å was used. The experimental data were corrected for background scattering and transformed into 1D-plots by azimuthal-angle integration using the FIT2D program developed

by Dr. Hammersley of ESRF. The resulting SAXS profiles were scaled for the sample thickness to allow a comparison of the intensities of different samples.

2.5. Dynamic mechanical thermal analysis (DMTA)

Rectangular samples with dimensions of around $10 \times 3 \times 1$ mm were measured over a temperature range from -100 to $250\,°C$ at a heating rate of $3\,°C/min$ and a frequency of 1 Hz on a DMA Q800 (TA Instruments) with film tension clamps.

2.6. Hardness

The hardness was measured on 6 mm thick samples using a Shore A durometer according to ASTM D2240–91.

2.7. Tensile testing

Dumbbell-shaped tensile bars with dimensions of $35 \times 2 \times 1$ mm and a parallel specimen length of 17.5 mm were punched from compression-molded films. Tensile tests were performed with a constant speed of 0.5 mm/s at room temperature on a Zwick Z010 tensile tester equipped with a force cell of 20 N using TestXpert v7.11 software. All materials were tested in at least five-fold.

2.8. Compression set (CS)

Cylindrical samples with a diameter of 13 mm and a thickness of around 6 mm were compressed for 22 h between two parallel plates with a linear deformation of 25% at room temperature (CS_{23}) or at $70\,°C$ (CS_{70}). CS was determined after a relaxation time of 30 min at room temperature using:

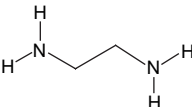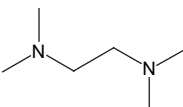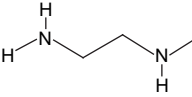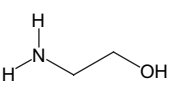$$CS = \frac{(t_0 - t_i)}{(t_0 - t_n)} \times 100\% \qquad (2)$$
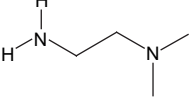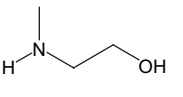
where t_n is the thickness of the spacer and t_0 and t_i are the initial and final sample thickness, respectively.
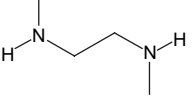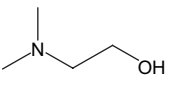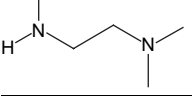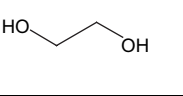
3. Results

3.1. Cross-linking of MAn-g-EPM

The MAn-g-EPM precursor is cross-linked in solution using equimolar amounts of the various di-functional cross-linkers with the same ethylene spacer, which are shown in Table 1 including their abbreviations. For comparison, the reactions with a diol (ethyleneglycol) is also studied. The chemical reactions of the cyclic anhydride groups of MAn-g-EPM with 1° or 2° amines in solution at room temperature are extremely fast even without a catalyst [22,32], resulting in immediate gelation for the 1°–1°, 1°–2° and 2°–2° cross-linkers. No significant differences were observed in the FTIR spectra of (many) different samples taken from the reaction product, which suggests that the gelation does not result in non-homogeneous materials. The reaction of the cyclic anhydride groups with the alcohol functionalities does not occur in solution even in the presence of a catalyst [24], so no gelation occurs in solution for the 1°–OH, 2°–OH, OH–OH and 3°–OH cross-linkers. Cross-linking only occurs after solvent evaporation and is catalyzed by a suitable catalyst (*p*-toluenesulfonic acid) for the diol (OH–OH cross-linker) [24] or by the amine groups [19] for the reactions with the 1°–OH, 2°–OH and 3°–OH cross-linkers. The solutions become somewhat more viscous for the reactions with the 1°–3°, 2°–3° and 3°–3° cross-linkers, due to the formation of ionic interactions after neutralization of the carboxylic acids.

Table 1
Overview of the different cross-linkers used in this study

Cross-linker	Name (abbreviation)	Cross-linker	Name (abbreviation)
	Ethylenediamine (1°–1°)		*N,N,N′,N′*-Tetramethyl-ethylenediamine (3°–3°)
	N-Methyl-ethylenediamine (1°–2°)		Aminoethanol (1°–OH°)
	N,N-Dimethyl-ethylenediamine (1°–3°)		2-(Methylamino)-ethanol (2°–OH°)
	N,N′-Dimethyl-ethylenediamine (2°–2°)		*N,N*-Dimethyl-ethanolamine (OH–3°)
	N,N,N′-Trimethyl-ethylenediamine (2°–3°)		Ethyleneglycol (OH–OH)

FTIR spectroscopy is a suitable technique to study these reactions, since the intensities of the carbonyl (C=O) stretching vibration bands of the cyclic anhydride groups at 1865 (weak) and 1785 cm^{-1} (strong) [22,29,33] decrease upon reaction and new C=O bands are present. The anhydride conversion (X_{Anh}) was calculated from the respective FTIR spectra (not shown here) using Eq. (1) and is given in Table 2. X_{Anh} was not determined for the cross-linkers with 3° amine groups, since the use of partially or fully hydrolyzed starting materials results in unreliable calculations. Conversions of approx. 80% and higher are obtained for the covalently cross-linked materials, indicating relatively high levels of cross-linking, with the exception of the 1°−2° cross-linker, which may be related to the very fast and, thus, inhomogeneous reaction within the highly viscous reaction medium.

Table 2 gives an overview of the new absorption bands for the cross-linked materials and the suggested chemical structures. Some absorption bands are broad, due to the presence of two overlapping bands. Two new, partially overlapping absorption bands at 1735 and 1710 cm^{-1} appear for the hemi-esters formed upon the reaction of cyclic anhydrides with alcohol groups, which originate from the C=O stretching vibrations of the ester and carboxylic acid groups, respectively [20,24]. The 1° amide−acid formed upon the reaction of cyclic anhydrides with 1° amines has absorption bands at 1710 cm^{-1} from the carboxylic acid groups and at 1640 and 1550 cm^{-1}, which are assigned to the C=O (amide-I) and N−H (amide-II) stretching vibrations of the amide groups, respectively, while the 2° amide−acid only has the carboxylic acid and amide-I bands [22,32]. Absorption bands are observed at 1710 and 1560 cm^{-1} upon neutralization with 3° amines, which originate from the C=O stretching vibrations of the carboxylic acid and carboxylate groups, respectively [33]. The broad amide-I bands for the 2° amide−acids (for the 1°−2°, 2°−2° and 2°−OH cross-linkers) suggest the presence of two different hydrogen-bonded species, possibly both intra- and inter-molecular hydrogen-bonded. In conclusion, Table 2 suggests that the expected reaction products are present for all cross-linked materials.

3.2. Reprocessability of the cross-linked materials via compression molding

It was shown in the previous section that the cross-linking reactions of the MAn-*g*-EPM precursor with all cross-linkers were successful. The question arises which of these materials are indeed reprocessable. For this purpose, the cross-linked materials were compression molded at 125, 150 and 175 °C. The materials compression molded at 175 °C were subsequently cut into small pieces (mm scale) and subjected to a second compression molding step at 175 °C. The resulting films were judged for their appearance, where a distinction is made between ''good flow'' (fully-fused, homogeneous films), ''sufficient flow'' (fused films with (some) defects) and ''poor flow'' (poorly-fused, heterogeneous films). The FTIR spectra of MAn-*g*-EPM cross-linked with the 1°−1°, 2°−2°, 3°−3° and OH−OH cross-linkers before and after compression molding are shown in Fig. 2.

The materials with covalent cross-links, involving only 1° and 2° amine and OH groups, do not flow sufficiently during compression molding at 125 °C to obtain defect-free materials. The respective equilibrium reactions with the anhydride groups are highly temperature-dependent and therefore higher temperatures were screened. Good flow is achieved for MAn-*g*-EPM cross-linked with OH−OH, 2°−2° and 2°−OH during compression molding at 150 and 175 °C and during the second compression molding step at 175 °C. The changes upon cross-linking for the OH−OH cross-linker are similar to those observed for short diols during the previous work [24], which are caused by the evaporation of the ethyleneglycol cross-linker. The second compression molding step for this materials was performed at 150 °C, since some irreversible di-ester formation occurs at 175 °C, as indicated by the decrease of the intensity of the carboxylic acid band compared to the ester band.

The FTIR spectra of MAn-*g*-EPM cross-linked with 2°−2° do not change significantly upon compression molding, except for the intensity ratios within the broad amide band centered around 1640−1630 cm^{-1}, which indicates that the ratio of the differently hydrogen-bonded amide groups changes (reversibility). The FTIR spectra for MAn-*g*-EPM cross-linked with 2°−OH (not shown here) are also not affected upon compression molding. These results demonstrate that no undesired (irreversible) side reactions occur for the 2°−2° and 2°−OH materials, which explains their good moldability.

MAn-*g*-EPM cross-linked with 1°−1° does not flow sufficiently at any of the compression molding temperatures.

Table 2
Overview of the absorption bands for the cross-linked materials and their (suggested) chemical structures

Cross-linker	X_{Anh} (%)	Ester	Acid	Amide-I	Carboxylate	Amide-II	Suggested structure(s)
1°−1°	82		1710	1641		1548	Amide−acid
1°−2°	67		1711	1640[a]		1545	Amide−acid
1°−OH	77	1737	1709	1642		1549	Amide−acid + hemi-ester
2°−2°	89		1713	1643[a]			(2°) Amide−acid
2°−OH	84	1736	1707	1634[a]			(2°) Amide−acid + hemi-ester
OH−OH	81	1739	1709				Hemi-ester
1°−3°	−		1709	1654	∼1560[a]	∼1560[a]	Amide−acid + carboxylate−acid
2°−3°	−		1713	1644	1569		Amide−acid + carboxylate−acid
OH−3°	−	∼1725[a]	∼1725[a]		1568		Hemi-ester + carboxylate−acid
3°−3°	−		1712		1568		Carboxylate−acid

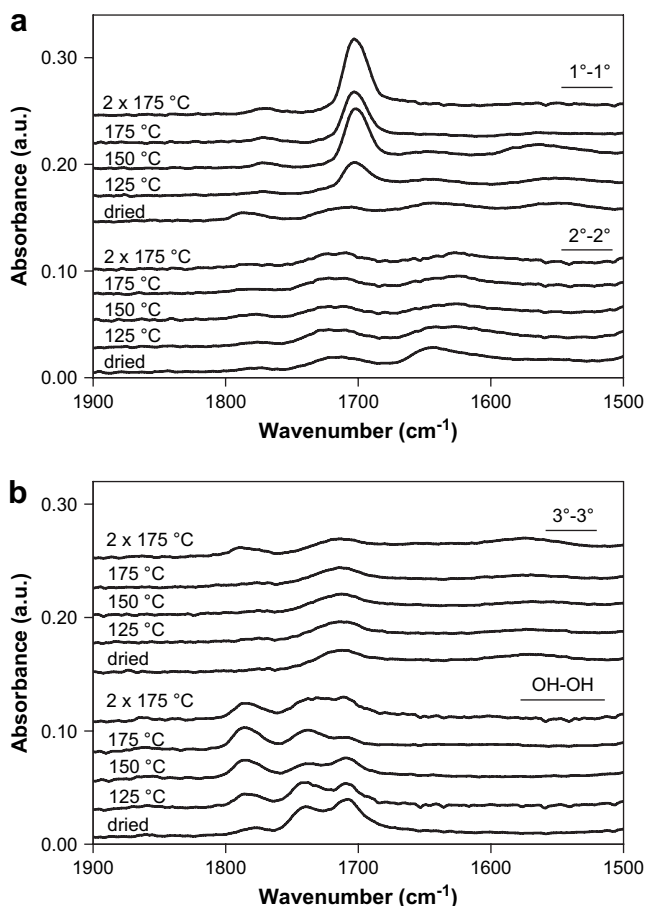[a] Broad overlapping absorption band centered at given value.

Fig. 2. FTIR spectra of MAn-*g*-EPM cross-linked with the (a) 1°–1° and 2°–2° and (b) 3°–3° and OH–OH cross-linkers before and after compression molding at various temperatures. The spectra are scaled on the EPM backbone band at 1460 cm⁻¹ and shifted vertically for clarity.

A large absorption band appears at 1705 cm⁻¹ after the first compression molding step and further increases in intensity after the second step, which originates from the C=O stretching vibration of the imide and indicates irreversible imide formation (Fig. 2a) [29,32]. The anhydride/1° amide–acid equilibrium allows some flow during the first compression molding step, although further flow is prevented by the (relatively fast) formation of irreversible (imide) cross-links. Imide formation occurs also for MAn-*g*-EPM cross-linked with 1°–2° and 1°–OH (FTIR spectra not shown here), resulting in the formation of irreversible imide connections between the cross-linker and MAn-*g*-EPM during the first compression molding step. Both materials do not flow sufficiently during compression molding, which suggests that reversibility of both parts of the cross-link is necessary to obtain flow under the current reprocessing conditions. A possible explanation for this behavior is that not enough cross-links are disconnected anymore to achieve sufficient flow.

The introduction of ionic interactions upon the addition of cross-linkers containing one or two 3° amine groups results in materials that flow very well at all compression molding temperatures. This is related to the relative weakness of ionic interactions with ammonium cations [31]. The FTIR spectra of

MAn-*g*-EPM cross-linked with 3°–3° (Fig. 2b) show that no significant chemical changes occur during the first compression molding step at any temperature, while the increase in the anhydride band during the second compression molding step at 175 °C may be related to the (partial) evaporation of the cross-linker (boiling point of 120 °C). The changes in the FTIR spectra for MAn-*g*-EPM cross-linked with 1°–3°, 2°–3° and OH–3° are similar to those of the corresponding functional groups of the 1°–1°, 2°–2° and OH–OH materials shown in Fig. 2. However, reversibility of the chemical bonds is not necessary for good flow of these materials, since the ionic interactions already allow good processability.

In conclusion, processable materials are obtained for (i) covalently cross-linked materials if no irreversible chemical reactions occur for both functional groups of the cross-linker (2° amine or OH), effectively excluding 1° amine groups, or (ii) materials with ionic interactions (at least one 3° amine). Furthermore, the reactions with the 2°–2° and 2°–OH cross-linkers result in covalently cross-linked materials that are repeatedly processable without chemical changes and therefore yield an improvement compared to cross-linking with diols (OH–OH cross-linker).

3.3. Morphology

SAXS experiments have shown that microphase-separated anhydride-rich aggregates are present in the MAn-*g*-EPM precursor [26]. The driving force for this aggregate formation is the large difference in polarity between the polar anhydride groups and the apolar EPM chains. The Yarusso–Cooper model [34] could describe the SAXS profiles of ionomers based on other MAn-*g*-EPM precursors very well [35]. However, fitting of the SAXS profiles of cross-linked materials based on the current MAn-*g*-EPM precursor is far from straightforward [25]. Therefore, in the context of this paper, no detailed structural description of the morphology is performed. Instead, the qualitative changes in the scattering curves are discussed, which is enabled by scaling the intensity for the sample thickness.

The SAXS profiles of the cross-linked materials after the first compression molding step at 175 °C are shown in Fig. 3. The scattering peak in the SAXS profiles remains for all cross-linked materials, indicating that the aggregates persist upon cross-linking. The intensity of the scattering peak increases in all cases compared to the MAn-*g*-EPM precursor, which is most probably related to a larger electron density difference between the aggregates and the matrix, due to the higher polarity of the reaction products compared to the original anhydride groups. The peak intensities are lower for MAn-*g*-EPM reacted with cross-linkers containing 1° amine groups, due to the lower polarity of the imide groups that were formed during compression molding.

For the covalently cross-linked materials (Fig. 3a), the peak maximum shifts to lower *q*-values for the cross-linkers with OH groups (OH–OH, 1°–OH and 2°–OH), whereas no significant shift occurs for those containing just 1° and 2° amine groups (1°–1°, 1°–2° and 2°–2°). This difference is most probably related to the use of the polar solvent THF during
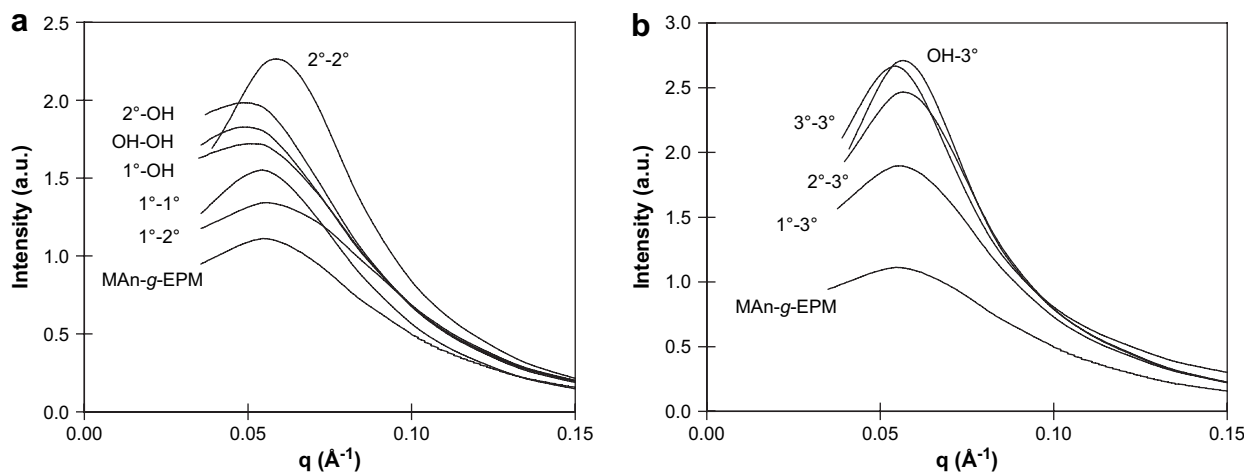
Fig. 3. SAXS profiles of MAn-*g*-EPM cross-linked with (a) covalent cross-links and (b) ionic interactions (combined with covalent bonds).

the cross-linking reactions, which results in the disappearance of the aggregates of the MAn-*g*-EPM precursor [36]. The cross-links are not formed in the solution for the cross-linkers containing OH groups, but only after solvent evaporation and, hence, in the presence of the aggregates. The formation of covalent cross-links occurs already in solution in the absence of aggregates for the cross-linkers containing only 1° and 2° amine groups. A tendency for aggregate formation exists after solvent evaporation, but the covalent network limits this process to a certain extent. Structural reorganization will occur during compression molding at elevated temperature, because of the increased mobility of the polymer chains segments and the (partial) disconnection of the cross-links. This may explain the observed differences in the peak maximum positions. The position of the peak maximum does not change significantly for the cross-linkers with 3° amine groups (Fig. 3b), most probably due to the relatively weak ionic cross-links.

DMTA experiments on the MAn-*g*-EPM precursor demonstrated that the aggregates act as physical cross-links that increase the network density compared to the parent EPM [25]. Fig. 4 shows the storage modulus as a function of temperature
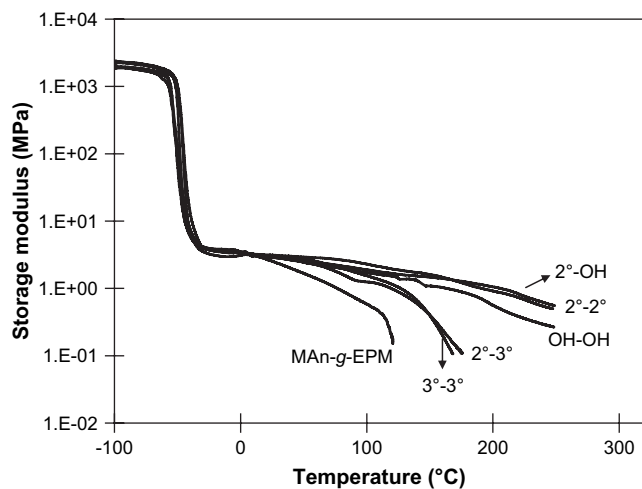
for MAn-*g*-EPM and some of the cross-linked materials. The 1°−OH material (not shown here) behaves similar to the 2°−2° and 2°−OH materials, while the 1°−3° material (not shown here) behaves similar to the 2°−3° and 3°−3° materials. The glass transition temperature positioned around −50 °C and the rubber plateau modulus do not change significantly upon cross-linking. The unaffected rubber plateau modulus indicates that the network density is not changed upon cross-linking and suggests that the covalent and ionic cross-links are only formed within the aggregates. The aggregates are strengthened by the introduction of ionic and covalent cross-links and therefore persist to higher temperatures, as indicated by the increased width of the rubber plateau upon cross-linking. A drop in the rubber modulus occurs around 160−170 °C for the materials with the relatively weak ionic interactions, which indicates the occurrence of flow, whereas only a gradual decrease in the rubber modulus occurs within the experimental temperature range (up to 250 °C) for the covalently cross-linked materials.

3.4. Mechanical properties

The mechanical properties of the cross-linked materials were determined after compression molding at 175 °C. The properties of the materials cross-linked with 1°−1°, 1°−2° and 1°−OH could not be determined, because the poor moldability resulted in inhomogeneous films. Representative tensile curves of the cross-linked materials are shown in Fig. 5, while Table 3 shows X_{Anh} after compression molding, as well as average values of the hardness, the tensile strength (TS), the elongation at break (EB), the modulus at 200% strain (M_{200}) and the compression sets (CS) at room temperature (CS_{23}) and at 70 °C (CS_{70}). CS is a measure for the elasticity of a material and has values of 0% for an ideally elastic material and of 100% for a fully plastic material. For materials containing (thermo) reversible interactions, CS depends on two (relaxation) processes, namely plastic deformation during the compression phase and elastic recovery after removal of the compression.

The properties of the materials cross-linked with 2°−2° and 2°−OH are comparable, but are different from those of the

Fig. 4. Storage modulus as a function of temperature for MAn-*g*-EPM cross-linked with the 2°−2°, 2°−OH, OH−OH, 2°−3°, and 3°−3° cross-linkers.
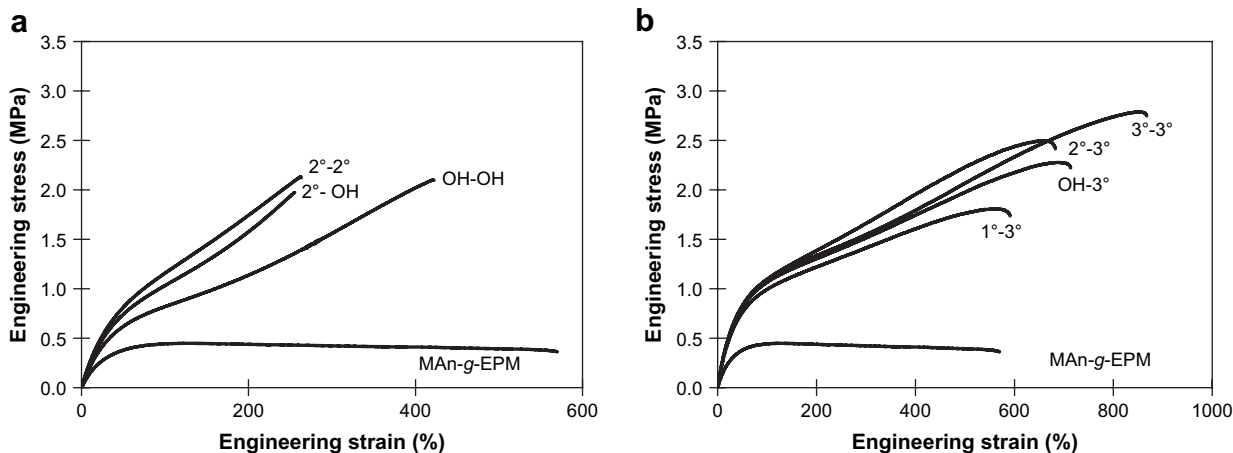
Fig. 5. Representative tensile curves for MAn-*g*-EPM cross-linked with (a) covalent cross-links and (b) ionic interactions. Note that the scales of the *x*-axes are different for clarity.

OH–OH cross-linker. This is related to the significantly lower X_{Anh} and, hence, lower level of cross-linking for the latter material, due to the aforementioned evaporation of the OH–OH cross-linker, whereas X_{Anh} decreases only slightly for the 2°–2° and 2°–OH cross-linkers after compression molding (compare Tables 2 and 3). This results in a significantly lower hardness and M_{200}, a higher EB and a lower (poorer) CS_{23} and CS_{70}, while the values of TS are comparable. Note that these trends are similar to the effect of the cross-link density on the rubber properties for covalently cross-linked elastomers [1]. The relatively poor CS_{70} for the 2°–2° cross-linker compared to the 1°–OH and 2°–OH cross-linkers may be related to the relatively fast anhydride/2° amide–acid equilibrium.

The use of ionic interactions instead of the covalent cross-links results in completely different mechanical properties. The higher EB and poorer CS for the materials with ionic interactions are all related to the occurrence of ion hopping [37]. This mechanism allows ionic groups to disconnect and to diffuse or "hop" between aggregates under deformation, which results in stress relaxation of the corresponding chains segments and prevention of premature failure, leading to higher values of EB. Obviously, hopping is not possible for the covalent cross-links, due to the extremely slow exchange kinetics at room temperature. For these materials, chemical bonds will break once the stress level becomes too high, resulting in early failure and, thus, a lower EB. Ion hopping causes significant plastic deformation during compression for the materials with ionic interactions, resulting in a higher CS than for the covalently cross-linked materials. This process becomes more prominent at higher temperatures, which results in high CS_{70} values close to 100%. The differences in tensile properties between the materials with ionic interactions are only small, except for the 1°–3° cross-linker, most probably due to the weaker aggregation with the less polar imide groups. The poorer CS_{23} and CS_{70} for the 1°–3° and 2°–3° cross-linkers compared to the 3°–OH and (especially) 3°–3° cross-linkers may be related to differences in the anhydride conversion, which could not be determined, as discussed previously.

3.5. Mechanism of (re)processability studied with FTIR spectroscopy

The materials containing ionic interactions could all be compression molded at temperatures as low as 125 °C, while the covalently cross-linked materials containing solely 2° amine or OH groups could be compression molded into homogeneous films at somewhat elevated temperatures of 150 and 175 °C. The moldability for the materials with ionic interactions results from "ion hopping", which is the generally accepted mechanism for the flow of ionomers [37,38]. Ionic groups can continuously disconnect and diffuse between aggregates, thereby allowing polymer chains to flow without breaking all ionic associations simultaneously. The relative weakness of the ionic interactions with ammonium cations, as demonstrated by all experiments in this study, allows flow via this mechanism already at relatively low temperatures.

The situation is different for the covalently cross-linked materials, for which the equilibrium reaction is responsible for the moldability. This is supported by the lack of flow for the 1°–1° cross-linker after the formation of an irreversible network. Previous work on the cross-linking of MAn-*g*-EPM with diols [24] demonstrated that the reversibility is not caused

Table 3
Mechanical properties of cross-linked materials compression molded at 175 °C

Sample	X_{Anh} (%)	TS (MPa)	EB (%)	M_{200} (MPa)	Hardness (shore A)	CS_{23} (%)	CS_{70} (%)
MAn-*g*-EPM	0	0.4	560	0.4	38	88	100
2°–2°	88	2.4	310	1.7	56	27	68
2°–OH	79	1.6	220	1.5	52	24	46
OH–OH[a]	56	1.9	400	1.1	48	31	64
1°–3°	–	1.8	590	1.2	50	56	100
2°–3°	–	2.5	680	1.4	54	56	100
OH–3°	–	2.3	700	1.3	55	50	92
3°–3°	–	2.8	830	1.3	52	44	88

[a] Material was compression molded at 150 °C.

by a shift in the reaction equilibrium at elevated temperatures, most probably due to the rather slow exchange kinetics and the occurrence of irreversible side reactions for some materials. Rather, a continuous, dynamic exchange between cross-linked and non-cross-linked species is thought to be responsible for the reprocessability. This exchange allows cross-links to continuously disconnect and re-connect, which gives the free functional groups and the corresponding chain segments freedom of movement and allows them to diffuse between the aggregates. This mechanism, which is quite similar to ion hopping [37,38], explained the flow of the diol-cross-linked MAn-*g*-EPM without a net equilibrium shift.

The mechanism of reversibility remains unclear from FTIR spectroscopy on the compression-molded samples, since the (chemical) changes during the actual compression molding step cannot be determined. Therefore, thin films of the cross-linked materials were subjected to the heating–cooling cycles under FTIR spectroscopy, as schematically depicted in Fig. 1. Fig. 6 shows the changes in the FTIR spectra for the 2°–2° cross-linker during such an experiment. The FTIR spectrum of the compression-molded film ($t = 0$ min) shows an absorption band at 1710 cm^{-1} for the carboxylic acid and two overlapping amide bands at 1648 and 1622 cm^{-1}. Note that their presence is much clearer for these experiments in transmission than for the ATR experiments in Fig. 2. During the first heating step at 175 °C, the intensity of the carboxylic acid band decreases, while the intensity of the anhydride band at 1785 cm^{-1} increases. The more or less unaffected total intensity of the two overlapping amide bands suggests that the total amount of amide groups does not change, although the ratio of peak intensities of the differently hydrogen-bonded amide groups changes. The FTIR spectra do not change significantly upon cooling to 50 °C, which shows that the changes during the first heating step are irreversible and that the (desired) shift in equilibrium from amide–acid to anhydride and amine does not occur. Rather, an irreversible reaction to form di-amide [22,30] and anhydride groups according to Scheme 2 seems to be responsible for the observed changes. This reaction may
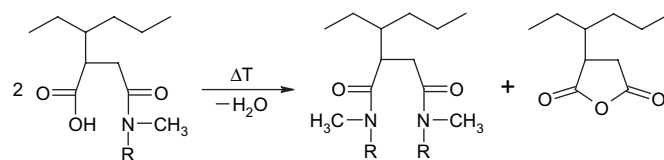
Scheme 2. Di-amide and anhydride formation from two amide–acids at elevated temperatures.

become more prominent at elevated temperatures and is irreversible due to the evaporation of water. No further chemical changes occur during the second heating–cooling cycle. These observations are different from those during compression molding, where no significant chemical changes occurred (Fig. 2). The reason for this may be that these heating/cooling experiments are performed in an open system, whereas the system is relatively closed during compression molding.

For the 2°–OH cross-linker (not shown here), the intensities of the ester and amide bands remain similar, while the anhydride band increases in intensity and the intensity of the carboxylic acid band decreases. Again, irreversible chemical reactions are responsible for these changes and not a shift in the anhydride/cross-linker equilibrium, since the FTIR spectra do not change further upon cooling. These changes can be attributed to the occurrence of both di-amide formation for the 2° amine groups (according to Scheme 2) and di-ester formation of the OH groups (according to Scheme 3) [24].

Although the changes observed during these heating/cooling cycles are different from those observed before and after compression molding, it can be concluded that similar processes occur for the 2°–2° and 2°–OH cross-linkers as for the cross-linking with diols [24] and that again a continuous, dynamic exchange between cross-linked and free groups is responsible for the flow of these materials.
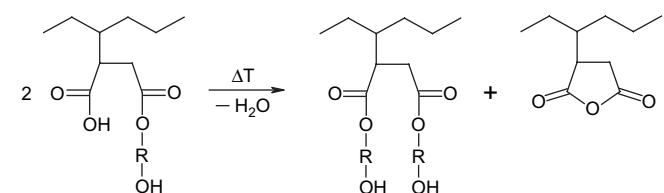
Scheme 3. Di-ester and anhydride formation from two hemi-esters at elevated temperatures.

4. Conclusions

The thermoreversible cross-linking of MAn-*g*-EPM with diamines and amino-alcohols was studied. The cyclic anhydride groups of MAn-*g*-EPM undergo reversible chemical reactions with 1° and 2° amine groups to form amide–acids and with alcohol groups to form hemi-esters. Cross-linkers with any combination of these functional groups results in the formation of covalent cross-links via the forward reaction at low temperature, if is used, while a shift of the equilibrium may result in their (partial) removal at elevated temperatures. Upon the neutralization of hydrolyzed anhydride groups with 3° amines, ionic
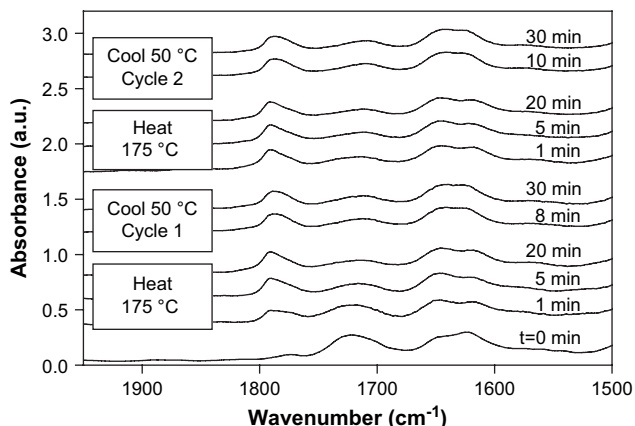
Fig. 6. FTIR spectra of MAn-*g*-EPM cross-linked with 2°–2° during two cycles of heating for 20 min at 175 °C followed by cooling for 30 min at 50 °C. The spectra are scaled on the EPM backbone band at 1460 cm^{-1} and shifted vertically for clarity.

interactions with ammonium cations are formed. FTIR spectroscopy confirmed the occurrence of the desired cross-linking reactions and showed that conversions of 80% or higher are obtained for the covalently cross-linked materials.

The use of cross-linkers with two 2° amine groups (2°–2°) and with 2° amine and alcohol (2°–OH) groups results in materials that are repeatedly processable via compression molding at 150 and 175 °C without chemical changes. This yields an improvement in reversibility compared to the previously-studied cross-linking with diols, for which irreversible side reactions did occur. The mechanical properties are also somewhat different for the 2°–2° and 2°–OH cross-linkers compared to the diol-cross-linked MAn-*g*-EPM, due to higher level of cross-linking for the former materials. Therefore, the use of the 2°–2° and 2°–OH cross-linkers is preferred above the use of the previously-used diols. FTIR spectroscopy suggested that their (re)processability originates from a continuous, dynamic exchange between cross-linked and free groups. The use of covalent cross-linkers containing 1° amine groups yields materials that are not reprocessable, due to irreversible imide formation. Finally, the introduction of ionic interactions (using 3° amine groups) results in materials that are easily (re)processable at temperatures as low as 125 °C and with significantly different mechanical properties than for the covalently cross-linked materials, all due to the occurrence of ion hopping.

Acknowledgements

References

[1] Hofmann W. Rubber technology handbook. Munich: Hanser Publishers; 1989.

[2] Holden G, Legge NR, Quirk RP, editors. Thermoplastic elastomers: a comprehensive review. Munich: Hanser; 1996.

[3] Engle LP, Wagener KP. J Macromol Sci Rev Macromol Chem Phys 1993;C33:239–57.

[4] Gheneim R, Perez-Berumen C, Gandini A. Macromolecules 2002;35:7246–53.

[5] Loiti E, Huglin MB, Rego JM. Macromol Rapid Commun 2003;24: 692–6.

[6] Kennedy JP, Castner KF. J Polym Sci Polym Chem Ed 1979;17: 2055–70.

[7] Salamone JC, Chung Y, Clough SB, Watterson AC. J Polym Sci Part A Polym Chem 1988;26:2923–39.

[8] Joel D, Hauser A. Angew Makromol Chem 1994;217:191–9.

[9] Hentschel T, Münstedt H. Polymer 2001;42:3195–203.

[10] Benecke HP, Markle RA. W.O. Patent 0192366 to Battelle Memorial Institute; 2001.

[11] Abbott NB, Chapman CB. US Patent 3,684,769 to Imperial Chemical Industries Limited; 1970.

[12] Van Pelt WWGJ. PhD thesis, Eindhoven University of Technology, Eindhoven, The Netherlands, 2001.

[13] Van Pelt WWGJ, Goossens JGP, Meijer HEH, Lemstra PJ. Polymer 2002;43:5699–708.

[14] Van Pelt WWGJ, Goossens JGP. Anal Chim Acta 2007;604:69–75.

[15] Pazos JF. US Patent 3,872,057 to E.I. du Pont de Nemours and Company; 1975.

[16] Wagener KB, Engle LP. Macromolecules 1991;24:6809–15.

[17] Augustin D, Leriche C, Poisson P. US Patent 4,617,354 to Atochem; 1986.

[18] Decroix JC, Bouvier JM, Roussel R, Nicco A, Bruneau CM. J Polym Sci Polym Symp 1975;52:299–309.

[19] Immirzi B, Laurienzo P, Malinconico M, Martuscelli E. J Polym Sci Part A Polym Chem 1989;27:829–38.

[20] Bruch M, Mäder D, Bauers F, Loontjens T, Mülhaupt R. J Polym Sci Part A Polym Chem 2000;38:1222–31.

[21] Hu GH, Lindt JT. J Polym Sci Part A Polym Chem 1993;31:691–700.

[22] Hu GH, Lindt JT. Polym Bull 1992;29:357–63.

[23] Schmidt-Naake G, Becker HG, Klak M. Macromol Symp 2001;163:213–34.

[24] Van der Mee MAJ, Goossens JGP, Van Duin M. J Polym Sci Part A Polym Chem 2008;46:1810–25.

[25] Van der Mee MAJ, l'Abee RMA, Portale G, Goossens JGP, Van Duin M. Macromolecules, submitted for publication.

[26] Sun CX, van der Mee MAJ, Goossens JGP, Van Duin M. Macromolecules 2006;39:3441–9.

[27] Aoyagi J, Shinohara I. J Appl Polym Sci 1972;16:449–60.

[28] Fedtke M, Pätz R. Acta Polym 1981;32:626–9.

[29] Vermeesch I, Groeninckx G. J Appl Polym Sci 1994;53:1365–73.

[30] Song Z, Baker WE. J Polym Sci Part A Polym Chem 1992;30:1589–600.

[31] Weiss RA, Agarwal PK, Lundberg RD. J Appl Polym Sci 1984;29: 2719–34.

[32] Schmidt U, Zschoche S, Werner C. J Appl Polym Sci 2003;87:1255–66.

[33] Lin-Vien D, Colthup NN, Fateley WG, Grasselli JG. The handbook of infrared and Raman characteristic frequencies of organic molecules. Boston: Academic Press; 1991.

[34] Yarusso DJ, Cooper SL. Macromolecules 1983;16:1871–80.

[35] Wouters MEL. PhD thesis, Eindhoven University of Technology, Eindhoven, The Netherlands, 2000.

[36] Van Duin M. Recent Res Dev Macromol 2003;7:1–28.

[37] Cooper W. J Polym Sci 1958;28:195–206.

[38] Vanhoorne P, Register RA. Macromolecules 1996;29:598–604.